Model of elastic responses of single DNA molecules in collapsing transition

Hirofumi Wada,* Yoshihiro Murayama, and Masaki Sano
Department of Physics, University of Tokyo, Hongo, Tokyo 113-0033, Japan
(Received 25 August 2002; revised manuscript received 25 October 2002; published 30 December 2002)

We present a simple phenomenological model to describe elastic responses of a collapsed single DNA molecule. The model is represented by the elastic theory for the wormlike chain combined with the order-parameter equation, which accounts for the intramolecular transition kinetics. Our continuum and discrete model reproduces the force plateaus and the stick-release patterns in the force-extension curves, respectively. Both of the elastic responses have been observed experimentally by changing the concentration of the condensing agents.

DOI: 10.1103/PhysRevE.66.061912 PACS number(s): 87.15.La, 64.75.+g

I. INTRODUCTION

Great advances in manipulating single macromolecules have enlightened rich and fascinating physics of biopolymers such as double-stranded DNA and actin filament. In particular, DNA condensation [1,2] has been the center of the concentrated efforts of many researchers in relation to the packaging of DNA in viruses and living cells. Single molecule observations by fluorescence microscopy have verified that individual DNA chains undergo a first-order phase transition from an elongated coil state to a collapsed globule state with the addition of various kinds of condensing agents such as multivalent cation [3,4]. It has been also observed by electron microscopy that a toroidal structure appears as an equilibrium collapsed state [5,6].

Another feature of these biopolymers can be found in its mechanical property. A stiffness of a molecule yields a characteristic elasticity. For a long DNA chain, the persistence length is typically of the order of 50 nm. Thus, it behaves as a random coil under good solvent condition, whereas a linear conformation is favored locally. Such a polymer is often called as a semiflexible polymer. In the low force regimes, an elastic response is almost the same as that of a long linear flexible polymer. However, a manifest deviation is found in the high force regime. The elastic property of a semiflexible polymer is now understood quantitatively in the framework of wormlike chain (WLC) model [7,8].

Thanks to huge amount of experimental and numerical studies, a rich store of knowledge on phase behavior and mechanical properties of a long DNA chain has been accumulated. But so far, the interplay between them has received limited attention. Our understanding of how the compaction of a single chain affects its mechanical properties is still poor.

Very recently, elastic properties of a collapsed DNA molecule have been investigated experimentally by some groups [9–11]. In our previous works [10,11] the elastic force of a single DNA molecule was measured using dual-trap optical tweezers in the coil-globule transition induced by a trivalent cation spermidine^{3+} (SPD). We found that the force versus extension curves showed two striking phases, i.e., force plateaus and stick-release patterns, depending on the concentration of SPD. When the concentration of SPD was 500 μM, the force plateau of 1–2 pN was observed during the polymer being both stretched and relaxed. When the concentration of SPD was in the higher range from 1 mM to 100 mM, stick-release patterns appeared in stretching processes, while force plateaus of 0.5–2 pN were observed only during relaxing. Besides, stick-release responses were obtained nearly periodically. This indicates subsequent abrupt unfolding of collapsed objects. Similar but more pronounced stick-release pattern was also found in stretching experiment of the giant sarcometric protein titin [12]. In this case, the periodicity arises directly from the modular structure of titin. Thus, the present case seems more difficult and profound because a single DNA molecule is structurally homogeneous before collapsing.

It is tempting to characterize the elasticity of a collapsed DNA theoretically. In this paper, we present a simple phenomenological model which can reproduce the measured force plateau and stick-release pattern in the force curves. Motivated by an analogy between a single DNA molecule condensation and a crystal growth from a supersaturated liquid [13], we adopt an order-parameter description to account for an intramolecular transition kinetics of a single chain.

In the following section, we introduce a continuum model describing a coil-globule transition in the presence of the external force. We restrict our interest to the force plateau in Secs. II and III. In Sec. III, we show by the numerical calculations that our model semiquantitatively reproduces the force plateau. In Sec. IV, we consider the discrete version of the model to investigate stick-release phenomena. Numerical calculations show that the modified model captures the experimentally measured trends of stick-release patterns. Discussions and possibility of further improvement of our model are presented with brief summary in Sec. V.

II. FORMULATION

A. Guidelines for modeling

Our goal is to calculate a force F of a collapsed DNA as a function of its extension x. Since the force F versus extension x relation is a thermodynamical one, an approach based on equilibrium statistical mechanics seems rather promising for our aim. As is well known, Marko and Siggia [8] derived

*Electronic address: wada@daisy.phys.s.u-tokyo.ac.jp

a force-extension formula for the ideal WLC by taking into account the bending elasticity of the polymer within the framework of equilibrium statistical mechanics. Its analytical expression is given by

$$F(x)=\frac{k_BT}{l_p}\left(\frac{x}{L}+\frac{1}{4(1-x/L)^2}-\frac{1}{4}\right), \tag{1}$$

where L is the contour length, l_p the persistence length, k_B the Boltzmann constant, and T the temperature.

However, the present situation seems quite different from the ideal case. In our case, elongated coils and compact globules coexist within a single molecule. In addition, transitions between a coil and a collapsed state can be induced by the externally applied force. For instance, when the chain is stretched by a larger force than the short-range attractive force for the compaction, some of globular objects undergo a conformational transition to a random coil. Furthermore, it is not suitable to expect that the system is kept in thermal equilibrium during stretching and relaxing. Thus, it is necessary to consider dynamical aspects of ordering processes of a single molecule under the external force.

To investigate such a complicated system, a phenomenological approach is often suitable. In this paper, we employ a Ginzburg-Landau-type phenomenology to describe the internal structure of a single polymer. Combining an equation for the order parameter with the formula Eq. (1) in a simple manner, we discuss the force-extension relation.

As already mentioned, experimentally measured force-extension curves showed plateaus and stick-release patterns depending on the depth of the condensation. It is not so easy, however, to construct a generic model which can describe both phases simultaneously. We consider the case of the force plateau at the first step. Next, by improving the model to suit the deep quench case, we will proceed to study the stick-release phenomena.

B. Model

When an intramolecular phase segregation has occurred and an elongated coil state and a collapsed state coexist within a single polymer, an apparent contour length L_a differs from the original one L_0 [14]. Presumably, the collapsed globule is hard to stretch compared to the coil. We then expect that the percentage of coil state mostly determines the flexibility of the polymer. If we identify this polymer with an ideal WLC having the contour length L_a, a force F and an extension x of the chain can be connected by the formula

$$F(x)=\frac{k_BT}{l_p}\left(\frac{x}{L_a}+\frac{1}{4(1-x/L_a)^2}-\frac{1}{4}\right). \tag{2}$$

Then what we have to do is to calculate "effective contour length" L_a under a given condition.

In this aim, we introduce an order parameter ρ along the coordinate s, where s is the contour distance from one chain end. We define that $\rho(s)ds$ represents the local contour length of coil-like flexible part within a small section $s\sim s+ds$ (see also Fig. 1). $\rho=1$ corresponds to a fully random coil state, while $\rho=0$ indicates an entirely collapsed state. In a bimodal state, ρ varies from 0 to 1. We assume that a collapsed part $(1-\rho)ds$ acts like a coil part with its length $\epsilon(1-\rho)ds$, where $\epsilon\ll 1$. This immediately leads to the following expression for the effective contour length:

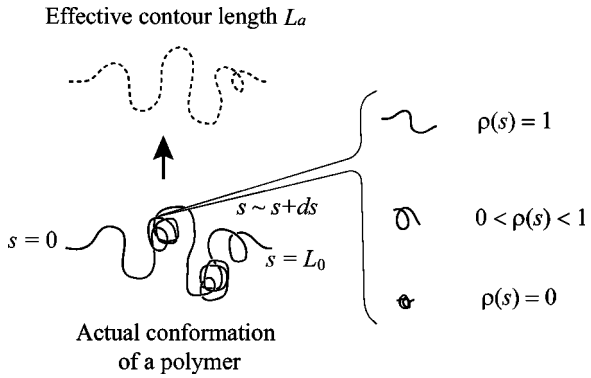

FIG. 1. Schematic illustration of the definition of the order parameter and the notion of the effective contour length.

$$L_a=\int_0^{L_0}\{\epsilon+(1-\epsilon)\rho(s)\}ds. \tag{3}$$

By the way, an ideal wormlike chain is nearly identical with a flexible polymer when ds is larger than the persistence length l_p. In such spatial resolution, the elasticity of the polymer is not noticeable. Therefore, we have to choose the magnitude of ds smaller than the persistent length. In the shallow quench case, a globule may be a so-called liquid blob rather than a crystal one because it is substantially swollen. Hence, it is conceivable to expect that an interface between coil and globule is well defined with its thickness ξ comparable to l_p. On the basis of these considerations, we determine $ds=\frac{1}{2}l_p$ here.

By the definition, ρ is a nonconservative quantity. We then assume that ρ obeys following relaxational dynamics:

$$\frac{\partial\rho}{\partial\tau}=-L\frac{\delta}{\delta\rho}(\beta H)+\eta(s,\tau), \tag{4}$$

where $\beta=1/k_BT$. The Gauss-Markov thermal noise η is assumed to be related to the kinetic coefficient L via the fluctuation-dissipation relation,

$$\langle\eta(s,\tau)\eta(s',\tau')\rangle=2L\delta(s-s')\delta(\tau-\tau'). \tag{5}$$

H is the coarse-grained Hamiltonian of the system and is written in the form

$$\beta H=\int_0^{L_0}\left\{\frac{c}{2}\left(\frac{\partial\rho}{\partial s}\right)^2+W(\rho,f)\right\}ds, \tag{6}$$

with a suitable upper cutoff wave number Λ. Here, W is an effective potential which includes the dimensionless force $f=l_pF/k_BT$ as a control parameter and has local minima at $\rho=0$ and $\rho=1$ for each f. The profile of W and its dependency on f are shown in Fig. 2. Here, a critical force value f_c is a material constant.

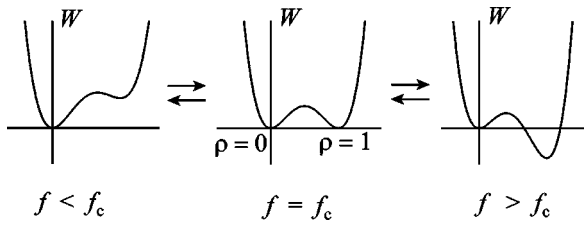

FIG. 2. Schematic representation of a double-well potential W controlled by the parameter f.

Choosing the polynomial form for W, we arrive at

$$h(\rho)=-\frac{\partial W}{\partial \rho}=\mu\rho(1-\rho)\left(\rho-\frac{1}{2}+k(f)\right), \tag{7}$$

where $|k|<1/2$. We assume that c and μ are positive constants for simplicity. $\Delta W=W(1,f)-W(0,f)=(\mu/6)k(f)$ is proportional to $f-f_c$, at least when f is close to f_c. On the other hand, ΔW approaches constant values $\pm(\mu/12)$ when f is away enough from f_c. Taking the numerical stability into account, we adopt the specific form of $k(f)$ as

$$k(f)=\frac{1}{2}\tanh\left(\frac{f-f_c}{v}\right), \tag{8}$$

where v is a material constant. In what follows, we will often use $b(f)=\frac{1}{2}-k(f)$ rather than $k(f)$ itself.

The equation of motion is now written as

$$\frac{\partial \rho}{\partial \tau}=D\frac{\partial^2 \rho}{\partial s^2}-\lambda\rho(\rho-b)(\rho-1)+\eta(s,\tau), \tag{9}$$

where we put $\lambda=\mu L$ and $D=cL$, which is the diffusion constant. Note that λ can be set to 1 by rescaling $\tau\rightarrow\lambda^{-1}\tau$. Also taking L_0 as the unit of space, the equation of motion is now expressed in the dimensionless form as

$$\frac{\partial \rho}{\partial \tau}=\nu^2\frac{\partial^2 \rho}{\partial s^2}-\rho(\rho-b)(\rho-1)+\theta(s,\tau), \tag{10}$$

with the fluctuation-dissipation relation

$$\langle\theta(s,\tau)\theta(s',\tau')\rangle=2M\delta(s-s')\delta(\tau-\tau'). \tag{11}$$

Here, $\nu^2=D/(\lambda L_0^2)=c/(\mu L_0^2)$ is the dimensionless diffusion constant, and $M=L/(\lambda L_0)=1/(\mu L_0)$ is the noise intensity. Note also that ν and M are now independent of the kinetic coefficient L.

Throughout this paper, we impose the zero-flux condition as the boundary condition of ρ:

$$\partial_s\rho(s=0,\tau)=0,\quad \partial_s\rho(s=1,\tau)=0. \tag{12}$$

C. Stationary solutions

One can readily find that Eq. (10) without the noise term has a stationary propagating solution satisfying the boundary condition $\rho(s\rightarrow\infty)=0$ and $\rho(s\rightarrow-\infty)=1$,

$$\rho(s,\tau)=\frac{1}{2}\left\{1-\tanh\left(\frac{s-U\tau}{\xi}\right)\right\}, \tag{13}$$

with the interface thickness $\xi=2\sqrt{2}\nu$ and the propagating velocity

$$U=\sqrt{2}\nu\left(\frac{1}{2}-b\right)=\frac{\sqrt{2}\nu}{2}\tanh\left(\frac{f-f_c}{v}\right). \tag{14}$$

For $b>\frac{1}{2}$, which is equivalent to $f<f_c$, the domain boundary (interface) is driven so that more stable region $\rho=0$ can expand, while for $b<\frac{1}{2}$, which is equivalent to $f>f_c$, the boundary moves in order to enlarge more stable region $\rho=1$. Only when the condition $f=f_c$ is kept for sufficiently long time, the whole system can reach the global thermal equilibrium. It is also noted that these analytic results are useful to check the validity of the numerical calculations which we perform in the following section.

III. NUMERICAL SIMULATION

A. Calculation methods

In the following simulations, we obtain F-x curves as a set of consecutive data points $(x_i,F_i),(i=1,2,\ldots,N_D)$ in stretching and relaxing processes, respectively. We always control the extension x_i and calculate the corresponding force F_i. In each measurement of (x_i,F_i), the extension is fixed at some value during a certain waiting time T_w after its instantaneous change. Since the force fluctuates during the waiting time T_w, we average the force for the waiting time in each measurement:

$$F_i=\frac{k_BT}{l_p}\left[\frac{1}{T_w}\int_0^{T_w}f(x_i,\tau)d\tau\right]. \tag{15}$$

The parameters are fixed at $L_0=5$ μm, $l_p=25$ nm, $T=296$ K corresponding to the setup of the experiment [11]. Since the thickness of the interface $\xi=2^{3/2}\nu$ is comparable to the scaled persistence length $l_p/L_0=5\times10^{-3}$, we have $\nu\sim10^{-3}$. The extension x is varied from $x_{min}=1.0$ μm to $x_{max}=4.8$ μm with $\Delta x=|x_{i+1}-x_i|$ set to 19 nm. The noise intensity M, the small parameter ϵ, material constants f_c and v are chosen to be 0.0005, 0.15, 12.5 and 3.7, respectively. The simulations are performed for the waiting time $T_w=2.5$ and 3.0. Unfortunately, we cannot specify the precise value of T_w in physical units because it is crucially dependent on the unknown kinetic coefficient L which has disappeared by the nondimensionalization. However, we have checked that $T_w=2.5$ and 3.0 are long enough for a polymer to reach quasistationary state for the above parameters by changing T_w from 0.5 to 3.5, whereas the data is not shown in this paper.

We use the standard implicit method (Crank-Nicolson scheme) for numerical integration by approximating the nonlinear term as

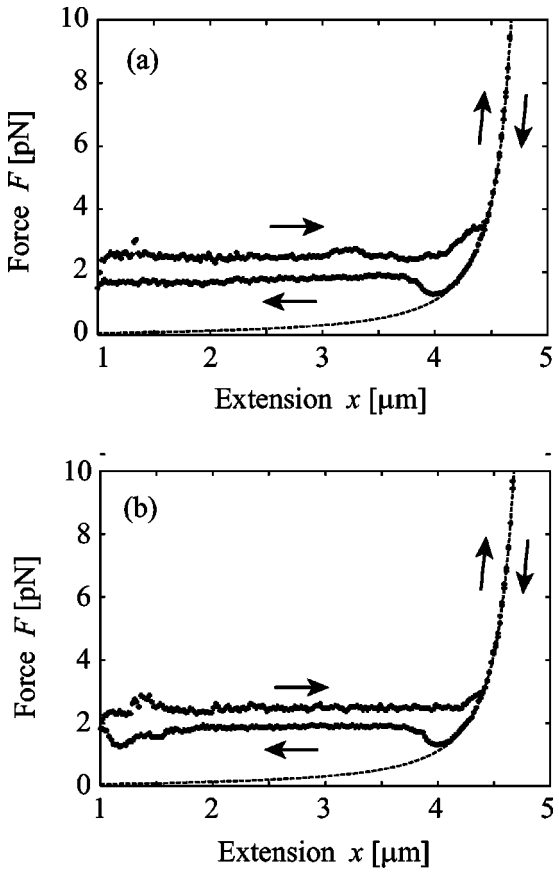

FIG. 3. Force versus extension curves. Parameters for these plots are (a) $M=5\times10^{-4}, \nu=0.001$, $f_c=12.5$, $v=3.7$, $T_w=2.5$; (b) the same as (a) except $T_w=3.00$. The dashed line is Eq. (1) with the parameters $l_p=25$ nm, $L=5$ μm, and $T=296$ K.

$$h[\rho(\tau+\Delta\tau)]\cong\frac{\rho(\tau+\Delta\tau)+\rho(\tau)}{2}[\rho(\tau)-b][1-\rho(\tau)], \tag{16}$$

with the time increment $\Delta\tau$ and grid size Δs set to 0.005 and 0.0025, respectively.

Throughout the following calculations, the initial condition of the chain is set to fully random-coil state $\rho=1$ with its extension $x_{max}=4.8$ μm. We first relax the polymer extension to $x_{min}=1$ μm, and again stretch it back to $x_{max}=4.8$ μm.

B. Force plateau

The calculated force versus extension curves are shown in Fig. 3. The simulation was performed with $T_w=2.5$ in Fig. 3(a), and with $T_w=3.0$ in Fig. 3(b), respectively. It is found that the elastic responses are obviously different from the WLC behavior. The F-x curves clearly show the force plateaus of 1–2 pN during both stretching and releasing processes. In the releasing process, a depression in the force curve can be seen associated with the onset of the force plateau. It is likely to be due to the nucleation barrier to generate a critical globule nucleus. In the stretching process, the plateau persists up to its extension ~4 μm, which is corresponding to 80% of its overall chain length. Moreover, a marked hysteresis appears between stretching and releasing processes. These features are also generically observed in the experiment [10,11]. One can find that the gap of the force plateaus between stretching and releasing processes in Fig. 3(b) seems to be narrower than that in Fig. 3(a). Further discussions of the physical mechanism underlying the emergence of hysteresis and its relation to the waiting time are given in the following section.

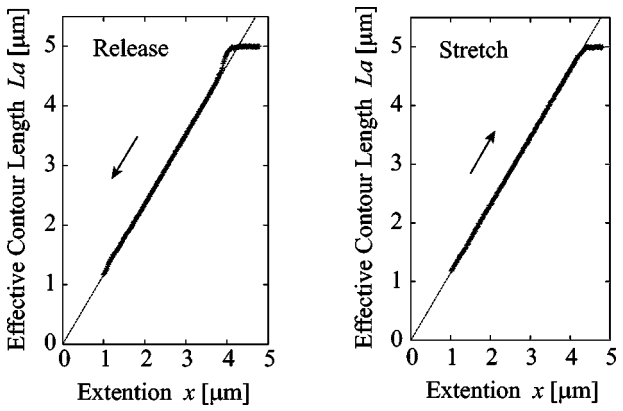

FIG. 4. Dependence of effective contour length L_a on the extension x in stretching and releasing processes for parameters as in Fig. 3(b). The dashed lines are $L_a=1.17x$ (release) and $L_a=1.15x$ (stretch), respectively.

Figure 4 shows the effective contour length L_a as a function of the extension x in the case of Fig. 3(b). One can clearly see that L_a is proportional to x while the force plateau is observed in Fig. 3. This can be understood intuitively by noticing that (dimensionless) force $f=f(z)$ remains constant as far as $Z\equiv x/L_a$ does not change in our model calculations. Figure 4 also suggests that the chain becomes fully elongated in $x>4.5$ μm, which is consistent with the WLC behavior found in $x>4.5$ μm in Fig. 3(b).

C. Hysteresis and motion of domain boundaries

In order to examine the nature of the hysteresis in force curves, let us consider the motion of domain boundaries in the one-dimensional s space. The profiles of $\rho(s)$ for several selected values of the extension x is displayed in Fig. 5 for parameters of Fig. 3(b).

Suppose now that there are N domains at time t. As shown in Fig. 6, a domain means a coil region in the s space, hereafter. We simply consider that there are $2N$ domain boundaries (interfaces) and their width is much smaller than the domain width. Note that the variable N can take a half of a natural number as well. Representing the interface positions of nth domain as $s=X_n^{(+)}(t), X_n^{(-)}(t)$, we can write down the equations of motion as

$$\frac{dX_n^{(+)}}{dt}=U(f), \tag{17}$$

$$\frac{dX_n^{(-)}}{dt}=-U(f), \tag{18}$$

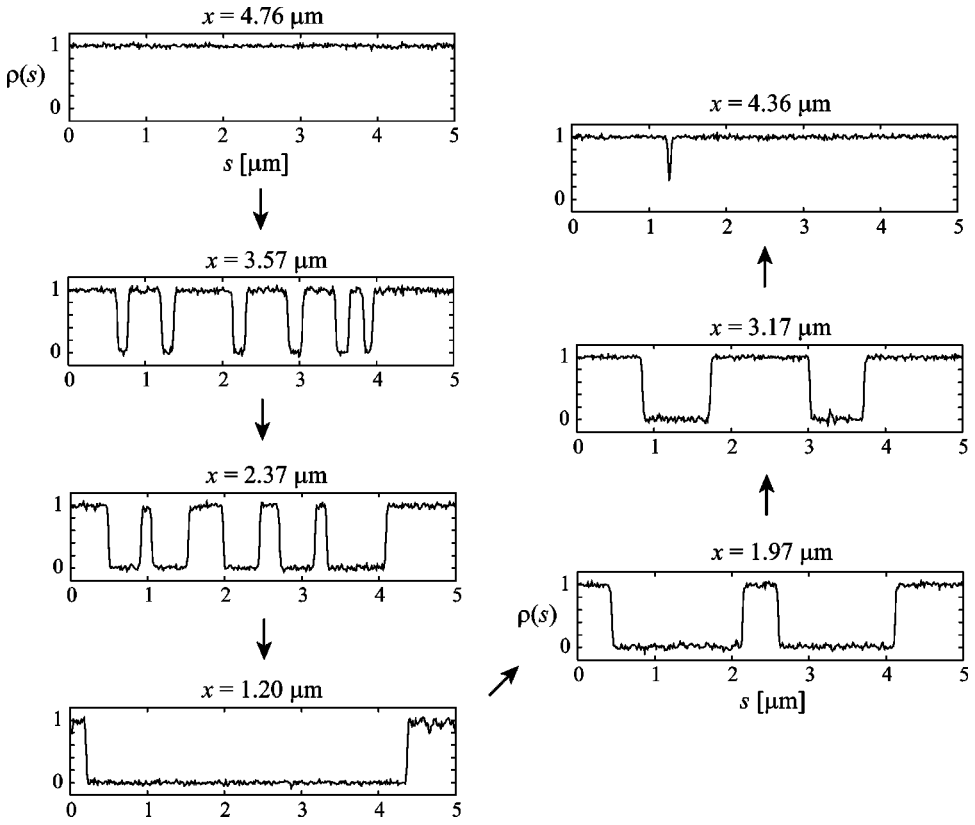

FIG. 5. Evolution of spatial domain structure along the polymer contour corresponding to the extension change. A series of these figures is obtained when the force curve is Fig. 3(b). The left hand side represents the releasing process from $x_{max}=4.8\ \mu$m to $x_{min}=1.0\ \mu$m, while the right hand side is the stretching process from $x_{min}=1.0$ to $x_{max}=4.8\ \mu$m.

where the velocity is given from Eq. (14) by

$$U(f)=U_0\tanh\left(\frac{f-f_c}{v}\right). \tag{19}$$

Let us consider the situation where the extension x is varied continuously as

$$x=x_0+\gamma t. \tag{20}$$

By exchanging the variable x from t, Eqs. (17) and (18) become

$$\gamma\frac{dX_n^{(+)}}{dx}=U(f), \tag{21}$$

$$\gamma\frac{dX_n^{(-)}}{dx}=-U(f). \tag{22}$$

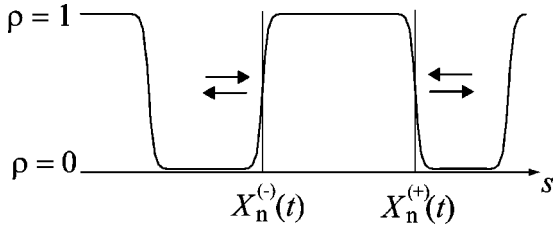

FIG. 6. Schematic illustration of the motion of domain boundaries.

Note that we have to choose $x_0=0$ and $\gamma>0$ in the stretching process, while $x_0=x_{max}$ and $\gamma<0$ in the releasing process. Then Eqs. (21) and (22) may hold in either stretching or releasing process.

Extracting Eq. (22) from Eq. (21), we obtain

$$\frac{d}{dx}(X_n^{(+)}-X_n^{(-)})=2\gamma^{-1}U(f). \tag{23}$$

In the force-plateau region, where the force f retains nearly constant value f_p, the velocity U is also constant at $U(f_p)\equiv U_p$. Since most of the domains disappear at $x=0$, $X^{(+)}-X^{(-)}\to 0$ can be realized in the limit of $x\to 0$. Solving Eq. (23) with this condition, we easily find

$$X_n^{(+)}-X_n^{(-)}=2\gamma^{-1}U_p x. \tag{24}$$

On the other hand, the apparent contour length can be calculated approximately in the limit of $\epsilon\to 0$ as

$$L_a\cong\int\rho(s)ds\cong\sum_n\ (X_n^{(+)}-X_n^{(-)}). \tag{25}$$

Substituting Eq. (24) into Eq. (25), we obtain

$$L_a=2N\gamma^{-1}U_p x. \tag{26}$$

Hence, we find that the quantity

$$Z=\frac{x}{L_a}=\frac{\gamma}{2NU_0}\left\{\tanh\left(\frac{f_p-f_c}{v}\right)\right\}^{-1} \tag{27}$$

is independent of the extension x. This gives the value of the slope of the dashed line in Fig. 4. This relation also provides us a self-consistent equation for f_p with the following formula:

$$f_p = Z + \frac{1}{4(1-Z)^2} - \frac{1}{4}. \tag{28}$$

Before solving Eqs. (27) and (28) in terms of f_p, we remark on some points. First, since the condition $Z<1$ should be satisfied at all times, the additional constraint for f_p is imposed by

$$\left|\frac{\gamma v}{2NU_0}\right| < \left| v \times \tanh\left(\frac{f_p - f_c}{v}\right)\right| < |f_p - f_c|. \tag{29}$$

Second, it should be noted that the number of domains N is a certain decreasing function of the stretching (or releasing) speed $|\gamma|$. In the limit of the quasistatic operation $\gamma \to 0$, a single-domain boundary may survive because the phase separation proceeds macroscopically in each x. Then, in order that the apparent contour length $L_a \sim 2xU_p/\gamma$ remains finite at $\gamma \to 0$, U_p also approaches zero as $\gamma \to 0$, which means that f_p coincides with f_c asymptotically in the quasistatic process.

So we restrict our interest to the small γ such that the following condition typically may hold:

$$\left(\frac{f_p - f_c}{v}\right)^2 \ll 1. \tag{30}$$

In this case, it is allowed to neglect the higher-order terms in the expansion $\tanh x \approx x + O(x^3)$. Setting $y = f_p - f_c$, we have following simultaneous equations:

$$Z(y) \cong \alpha y^{-1} \tag{31}$$

and

$$y = Z(y) + \frac{1}{4[1-Z(y)]^2} - \beta, \tag{32}$$

where we put $\alpha = \gamma v/2NU_0$ and $\beta = f_c + 1/4$. The constraints (29) and (30) may be expressed together as

$$|\alpha| < |y| \quad \text{and} \quad (y/v)^2 \ll 1. \tag{33}$$

Substituting Eq. (31) into Eq. (32), we obtain the equation for y as

$$p(y) = y^4 - \left(2\alpha - \beta + \frac{1}{4}\right)y^3 + (\alpha^2 - 2\alpha\beta - \alpha)y^2 + \alpha^2(\beta+2)y - \alpha^3 = 0. \tag{34}$$

We first investigate the schematic profile of the function $p(y)$. We readily find $p(0) = -\alpha^3$, $p(\alpha) = -\alpha^3/4$, $p'(0) = \alpha^2(\beta+2)$, and $p'(\alpha) = -3\alpha^2/4$, where the prime denotes the derivation with respect to y. Therefore, for positive α, Eq. (34) has a solution in $y<0$, a local maximum somewhere in the region $0<y<\alpha$, and a desired solution in $y>\alpha$, respectively. We represent this solution as $y = \Delta_>$. On the other hand, we find that there is only one solution in $y<\alpha$ which satisfies the constraint (33) for reasonable negative values of α and for β used in the above simulations. We express this solution as $y = -\Delta_<$.

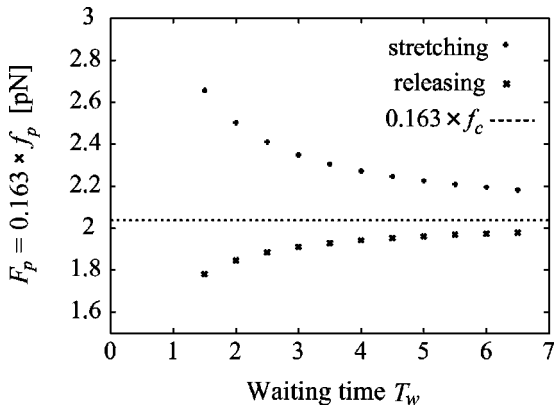

FIG. 7. The magnitudes of force plateaus in stretching and releasing processes given as the solutions of Eq. (34).

As a consequence, the magnitudes of the force plateaus are given by

$$f_p^{stretch} = f_c + \Delta_>, \tag{35}$$

for stretching process ($\alpha>0$), and

$$f_p^{release} = f_c - \Delta_<, \tag{36}$$

for releasing process ($\alpha<0$). Thus the finite force gap $\Delta = f_p^{stretch} - f_p^{release} = \Delta_> + \Delta_<$ generally exists for nonzero α. This directly suggests that the hysteresis appears in the force curve during stretch and release processes. However, in the quasistatic limit $\alpha \to 0^{\pm}$, Eq. (34) simply becomes

$$y^3(y + f_c) = 0. \tag{37}$$

Thus, the trivial solution $y=0$, namely, $f_p = f_c$ only survives. Because we immediately have $\Delta = 0$ in this case, no hysteresis appears in the force curve, at least apart from the initial transient regime of the onset of the plateaus.

We solved Eq. (34) numerically by changing the stretching and releasing speed γ. The results are shown in Fig. 7. Actually the magnitude of γ is represented by the waiting time T_w, which is related to γ as $\gamma = |\Delta x|/T_w$. We set $|\Delta x| = 3.8 \times 10^{-3}$ corresponding to the simulations in Fig. 3. We also substitute $N(\gamma)$ with the average number of domains $\overline{N}$. Judging from Fig. 5, we set $\overline{N} = 2$ in the stretching process and $\overline{N} = 5$ in the releasing process, respectively. Note that the dimensionless value f_p is converted to the real force value F_p as $F_p = 0.163 \times f_p$ in Fig. 7. The predicted values of F_p by the present simple analysis are very close to those obtained in the simulations as summarized in Table I. The calculation also predicts that the force gap decreases with increase of the waiting time, and vanishes in the long waiting time limit. This implies that the polymer essentially under-

TABLE I. The magnitudes of force plateaus in stretching and releasing processes obtained by Eq. (34) and by the simulations. The values from the simulations averaged between $x=2$ μm and $x=3$ μm.

	$T_w=2.5$	$T_w=3.0$
$F_p^{stretch}$ (simulation)	2.48	2.48
$F_p^{stretch}$ (prediction)	2.41	2.35
$F_p^{release}$ (simulation)	1.76	1.90
$F_p^{release}$ (prediction)	1.88	1.91

goes nonequilibrium phase transition when it is stretched or relaxed with a finite speed, whereas its conformational transition recovers equilibrium reversibility only in the quasistatic operation limit. Although such a consideration is also expected from the simple thermodynamical argument, to confirm this statement, one may require a more detailed study due to the complexity of the present system. They will be reported elsewhere.

IV. STICK-RELEASE PHENOMENA

A. Modular structure

When the concentration of multivalent cation is large enough to induce deep condensation of a single polymer, the force-extension curves show stick-release patterns. In the experiment [11], there is a tendency for the stick-release response to occur periodically with a certain characteristic length $l_u \sim 300$ nm. We immediately associate this finding with a beaded structure, where a few ''crystallized'' globular objects are connected with short coils (see also Fig. 8). Such a morphology has been actually observed by fluorescence microscopy in a long DNA chain collapsed but partially stretched by the externally applied electric field [13]. Provided that the chain takes such a beaded structure, stick-release responses correspond to subsequent abrupt release of condensed objects. Furthermore, since l_u is comparable to the length of one turn of toroid [5,6], we empirically consider that a globular bead forms a toroidlike structure with its typical size $d \sim 100$ nm. It is considered that such an intramolecular phase segregated state is thermodynamically stable. Some authors have observed such a state that compact domains with their typical sizes d remain stable without further aggregations [4,13]. However, to answer the question that why such a unique structure is generated within a single molecule is beyond the scope of this paper. Instead, we solely give a rather simplified description of the stick-release phenomena and show that qualitatively similar elastic responses can be reproduced by slightly modifying our plateau model.

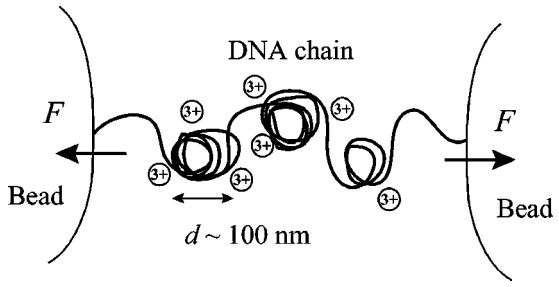

FIG. 8. Schematic illustration of an intramolecular phase segregated chain as an image.

From these considerations, let us employ further coarse graining of the spatial structure of the polymer. The characteristic length is not the persistence length l_p as opposed to the force plateau, but the diameter d of the compact globular object in the real space. We expect that the order parameter $\rho(s)$ is constant, at least within the distance l_u along s. Moreover, the interface between $\rho=0$ and $\rho=1$ may be very steep. We then assume that the chain is composed of $Q=L_0/l_u$ pieces of ''modules'' that can undergo a transition between two energetically different states. Although this idea is originally inspired by the work of Rief *et al.* [15] for the muscle protein titin, whether such a modular structure is spontaneously formed is less pronounced in a collapsed DNA chain. In case of the DNA chain, there is relevant short-range interaction between polymer segments to recover structural uniformity. Such an effect can be partially responsible for the formation of a compactly packed toroidal structure. We thus let the diffusion constant ν be finite in the present model.

On the basis of these preparations, let us improve our model to suit the present situation. The procedure is simply as follows:

$$\rho(s,\tau) \to \rho_i(\tau), \qquad \int_0^{L_0} ds \to l_u \sum_{i=1}^{Q} . \tag{38}$$

This is the discrete version of the plateau model. A conformational transition mainly occurs when it is thermally activated.

B. Simulation results

Numerical simulations were performed with the parameters $Q=16$, $\epsilon=0.10$, and $M=5-6\times10^{-5}$. It is legitimate here to choose a smaller value of M than that for the force plateau because the effective potential W has deeper minima in the collapsed phase. Other conditions are the same as those of the preceding section.

A selected plot of the elastic responses are shown in Fig. 9. In stretching processes, stick-release-like patterns appear, while the force plateaus of 0.5–2 pN in magnitude are observed during relaxing process. Force magnitudes at the peak positions are generally within the range of 4–12 pN. Hence, the main features of our previous measurements on elastic response of a collapsed DNA [11] are reproduced by the present numerical calculations for reasonable values of the dimensionless parameters.

In Fig. 10, we plot the effective contour length L_a as a function of the extension x for parameters of Fig. 9(a). The curve $L_a=L_a(x)$ looks rather irregular compared to that of a force plateau. Sharp changes of the contour length may correspond to abrupt releases of the globular objects or rapid

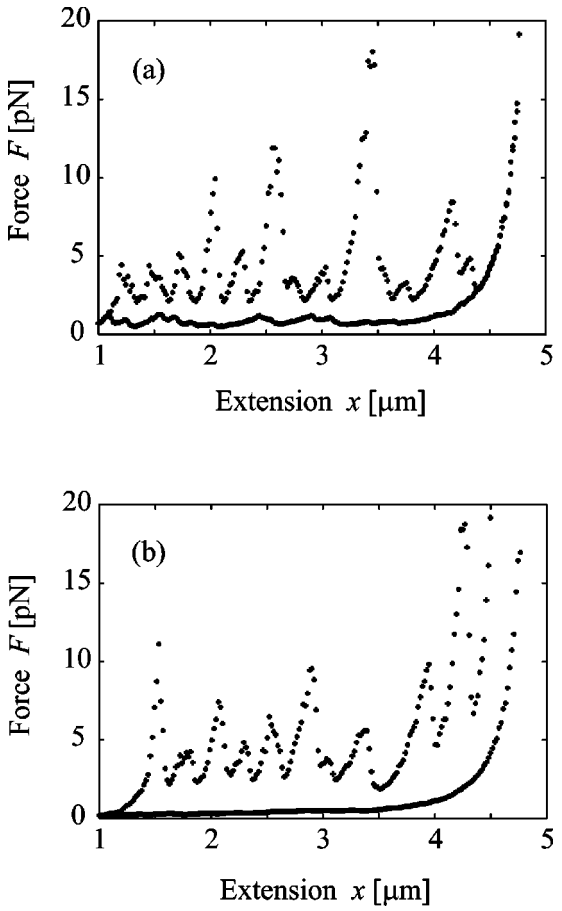

FIG. 9. Force versus extension curves. Parameters for these plots are (a) $M=6\times10^{-5}$, $\nu=0.001$, $f_c=12.0$, $v=6.0$, $T_w=3.0$ (b) $M=5\times10^{-5}$, $\nu=0.001$, $f_c=12.0$, $v=8.0$, $T_w=2.5$.

condensations of narrow coils. Hysteresis in the L_a versus x curve is more evident than that of the force plateau, which reflects the larger irreversible work in the cycle process as can be seen from Fig. 9.

Lastly, we show the profile of $\rho(s)$ for several selected values of the extension x in Fig. 11 for parameters of Fig. 9(a). Apart from the regions near domain boundaries, the overall structure and its evolution are, at first sight, similar with those of the force plateau. The structure emerged in the column of $x=1.20$ μm can be interpreted as the expected beaded structure. However, because of the shortness of the original contour length, a beadlike structure seems to be difficult to appear in the present case on the whole. A larger amount of toroidal object would be generated provided that the chain is much longer. To our knowledge, there is no experimental report to study whether such a morphology is actually formed when the chain is stretched by the mechanical stress. It is of great interest and one of the present authors is now conducting the experiment to clarify this question.

V. DISCUSSION AND SUMMARY

Our theoretical calculations suggest that two types of elastic responses, i.e., force plateau and stick-release pattern can be understood as WLC behavior of an apparent contour

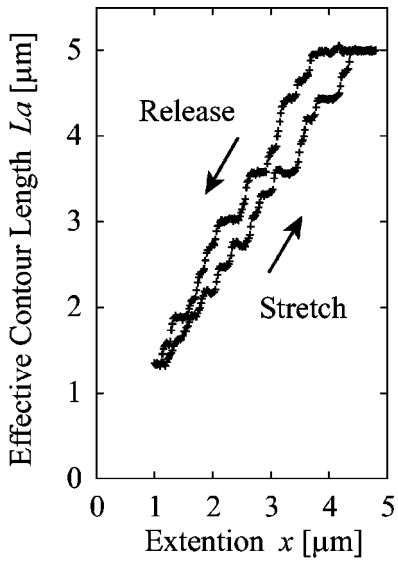

FIG. 10. Shown are extension dependence of effective contour length L_a in the forward and reversed process for parameters as in Fig. 9(a).

length which can vary with the force dependent transition rate. It is proved that combining the elastic theory of a single polymer with the kinetics of a metastable system is efficient to describe the main features of the measured force-extension curves of a collapsed DNA. In particular, the continuum model with diffusion along the chain is suitable for describing a force plateau. The motion of domain boundaries, which can be induced by the force working on the chain, is important to understand the plateau in force curves. We also found from the simple analysis that hysteresis is generically appreciable for finite stretching speed, while it is expected to vanish in the quasistatic limit. This implies that the system is generally in the nonequilibrium process in the stretching experiment. On the other hand, a steep change in the measured force may involve an abrupt and cooperative transition from a globular state to an elongated coil state. Therefore, a modular structure seems to be an essential ingredient for the stick-release pattern. Although there is no consensus of this suggestion, our calculations based on the discrete model strongly supports this idea.

Here we refer to the dimensionality of the system briefly. In the present study, we considered the one-dimensional system and only took into account the closeness due to the connection between segments along the chain. However, since the polymer is embedded into a three-dimensional system, it is generally possible for a segment to have contact with other segments which are separated along the chain. Such a contact may become a trigger for further growth of a condensation when the chain is in the metastable state under a poor solvent condition. Thus, the dimensionality is an important problem, in general, to consider a coil-globule transition [14]. In our case, however, both the ends of the polymer are trapped at controlled positions and the chain is forced to stretch with shorter apparent contour length than the original one. Then the polymer is considered to be rather

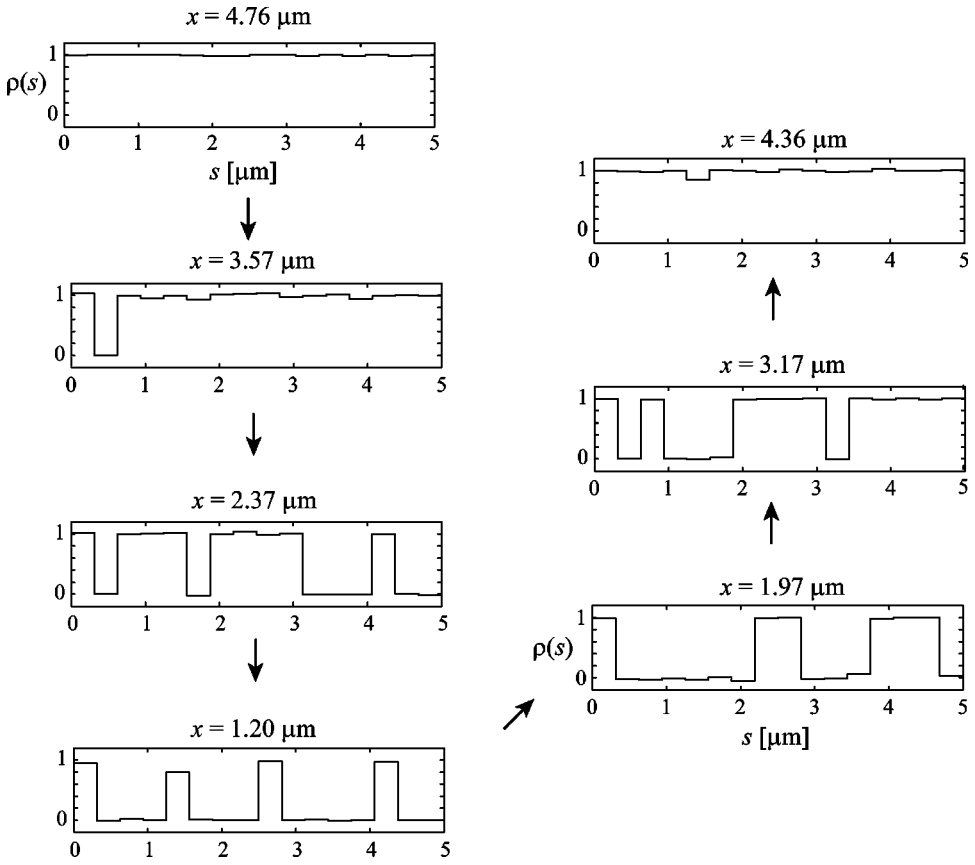

FIG. 11. Evolution of spatial domain structure along the polymer contour corresponding to the extension change. A series of these figures is obtained when the force curve is Fig. 9(a). The left hand side represents the releasing process from $x_{max}=4.8\ \mu$m to $x_{min}=1.0\ \mu$m, while the right hand side is the stretching process from $x_{min}=1.0$ to $x_{max}=4.8\ \mu$m.

''straight'' almost throughout the measurements. In such situations, a nucleation primarily occurs by the contact among nearby segments along the chain. Thus, our one-dimensional model is expected to be fairly appropriate.

Regardless of the satisfactory agreements between our theoretical calculations and experimental results, it should be still concerned that our present model is somewhat oversimplified, especially for the stick-release phenomena. In this paper, we applied slightly different models to describe force plateaus and stick-release responses, respectively, which may be eventually the source of our uneasiness. We assumed the attractive force between polymer segments from the beginning by preparing the double-well potential W for the chain conformation. In order to avoid any complexity and to emphasize on the influence of the condensation of a DNA molecule on its mechanical property, we did not consider the electrostatic effects explicitly. However, since a DNA molecule is highly charged with negative charges and a nearly 90% charge neutralization by the counterions is needed for the DNA condensation to occur [16], electrostatic effects are intrinsically most important in determining the conformation of a DNA. Many attempts have been made so far [17–20] to clarify the counterion induced attraction between two parallel charged rods as a model of the condensation of charged macromolecules, and some of them seem quite promising now. But they cannot be directly applied to the problem of the condensation of biopolymers, mainly due to the lack of knowledge on the delicate molecular architecture of biopolymers [20]. Then, for more realistic problem such as a DNA condensation induced by multivalent cations, many conceptual questions still remain (even when the polymer is not subjected to any mechanical stress). Hence, it offers further complicated problem of how and why a collapsed DNA chain forms the unique modular structure under load [11]. There may be a lot of important ingredients to be considered, such as the competition between long-range Coulombic repulsion and short-range attraction between segments, or the gain of translational entropy by the exchange between monovalent and multivalent cations [4]. Besides, not only these electrostatic-originated effects but also dynamical couplings between them and the conformational change due to external stress may enter into our problem.

Although the situation seems rather difficult as mentioned just above, it is still challenging to develop an elaborate description on the observed stick-release phenomena. Encouraged by the good agreement between our present phenomenological model and the experimental observations, we further expect that it is a promising way to introduce another order parameter in order to account for these electrostatic effects, as well as the current order parameter ρ. On the basis of this prospect, constructing a two-order-parameter description on the DNA condensation is in progress.

ACKNOWLEDGMENTS

We are grateful to Takao Ohta for a number of helpful discussions, especially on the motion of domain boundaries. We also acknowledge Shin-ichi Sasa for his variable comments.

[1] L.C. Gosule and J.A. Schellman, Nature (London) **259**, 333 (1976).
[2] R.W. Wilson and V.A. Bloomfield, Biochemistry **18**, 2192 (1979).
[3] K. Yoshikawa, M. Takahashi, V.V. Vasilevskaya, and A.R. Khokhlov, Phys. Rev. Lett. **76**, 3029 (1996).
[4] S. Takagi, K. Tsumoto, and K. Yoshikawa, J. Chem. Phys. **114**, 6942 (2001).
[5] P.G. Arscott, A.-Z. Li, and V.A. Bloomfield, Biopolymers **30**, 619 (1990).
[6] G.E. Plum, P.G. Arscott, and V.A. Bloomfield, Biopolymers **30**, 631 (1990).
[7] C. Bustamante, J.F. Marko, E.D. Siggia, and S. Smith, Science **265**, 2599 (1994).
[8] J.F. Marko and E.D. Siggia, Macromolecules **28**, 8759 (1994).
[9] C.G. Baumann, V.A. Bloomfield, S.B. Smith, C. Bustamante, M.D. Wang, and S.M. Block, Biophys. J. **78**, 1965 (2000).
[10] Y. Murayama and M. Sano, J. Phys. Soc. Jpn. **70**, 345 (2001).
[11] Y. Murayama, Y. Sakamaki, and M. Sano, Phys. Rev. Lett. (to be published).
[12] M. Rief, M. Gautel, F. Oesterhelt, J.M. Fernandez, and H.E. Gaub, Science **276**, 1109 (1997).
[13] M. Ueda and K. Yoshikawa, Phys. Rev. Lett. **77**, 2133 (1996).
[14] K. Yoshikawa and Y. Matsuzawa, J. Am. Chem. Soc. **118**, 929 (1996).
[15] M. Rief, J. M. Fernandez, and H. E. Gaub, Phys. Rev. Lett. **81**, 4764 (1998).
[16] V.A. Bloomfield, Biopolymers **44**, 269 (1997).
[17] F. Oosawa, Biopolymers **6**, 1633 (1968).
[18] G.S. Mannning, Q. Rev. Biophys. **II** , 179 (1978).
[19] B.-Y. Ha and A.J. Liu, Phys. Rev. Lett. **79**, 1289 (1997).
[20] N. Grønbech-Jensen, R.J. Mashl, R.F. Bruinsma, and W.M. Gelbart, Phys. Rev. Lett. **78**, 2477 (1997).